Available online at www.sciencedirect.com

ScienceDirect

Procedia Chemistry 3 (2011) 122–131

Chemistry Procedia

22nd Solvay Conference on Chemistry

Excitation of Biomolecules by Coherent vs. Incoherent Light: Model Rhodopsin Photoisomerization

Kunihito Hoki[a,b], Paul Brumer[b]

[a]*Department of Chemistry, Graduate School of Science, Tohoku University, Sendai, Miyagi 9808578 Japan*
[b] *Chemical Physics Theory Group, Department of Chemistry, and Center for Quantum Information and Quantum Control, University of Toronto, Toronto, Canada M5S 3H6*

Abstract

Light-induced processes in biological molecules, which occur naturally in continuous incoherent light, are often studied using pulsed coherent light sources. With a focus on timescales, the relationship between excitation due to these two types of light sources is examined through a uniform minimal model of the photoisomerization of retinal in rhodopsin, induced by either coherent laser light or low level incoherent light (e.g. moonlight). Realistic timescales for both processes are obtained and a kinetic scheme involving rates for both coherent and incoherent light excitation is introduced, placing all timescales into a uniform framework. The rate limiting step in the natural light-absorption process is shown to be the low incoherent photon flux.

Keywords: incoherent light, coherent laser light, photoisomerization, biological molecules, retinal, rhodopsin

1. Introduction

Developments in fast pulsed lasers have allowed for detailed time dependent studies of photobiological processes such as laser induced *c*is/trans isomerization of retinal in rhodopsin , giving the first step in vision [1, 2, 3, 4, 5], or electronic energy transfer in light harvesting proteins [6, 7, 8, 9]. Increasingly sophisticated coherent laser spectroscopies have been utilized to gain deeper insights [6, 7] into the processes. However, photoinduced processes such as these occur in nature in the presence of weak incoherent light, rather than in the strong coherent light that emanates from laser sources. For example, photoabsorption in rhodopsin initiates vertebrate visual transduction in dim light, such as moonlight [10]. The processes induced by these two types of sources are qualitatively different [11, 12, 13]. Significantly, in isolated systems, pulsed coherent light induces time dependent molecular dynamics, whereas purely incoherent light does not. Hence, it is important to establish the relationship between them.

Although this issue is of general interest to a wide variety of examples in light-induced dynamics, we address it here for the case of the photoisomerization of retinal in rhodopsin induced by a single femtosecond laser or by incoherent moonlight. The process itself is of particular biological interest due to the large quantum yield (~ 65 %), high speed (~ 200 fs) of reaction, and importance in the function of living organisms [1, 2, 3, 14]. We emphasize that *qualitative* features of the results are also relevant to studies of other photoexcited biological systems.

In the case of light absorption in rhodopsin, the primary interest of most laser excitation studies has been the timescales over which the subsequent retinal photoisomerization occurs. For this reason we focus below on temporal issues under both coherent and incoherent excitation. In doing so we have adopted a *minimalist* model of light

1876–6196 Selection and/or peer-review under responsibility of G.R. Fleming, G.D. Scholes and A. De Wit
 doi:10.1016/j.proche.2011.08.019

induced biological isomerization, justified by the fact that our specific focus is to address effects due to coherent vs. incoherent light. Specifically, below we provide a uniform minimal model for retinal photoisomerization induced by either coherent or incoherent light. The model has: (a) a computed dynamics timescale for femtosecond laser pulse excitation in agreement with experiment, (b) realistic dynamics for time scales on the order of milliseconds for moonlight induced processes, and (c) a kinetic scheme involving rates of both incoherent and coherent excitation that places all timescales within a unified framework. Specifically, in the natural visual process, the femtosecond coherent timescales provide the initial rise of the *cis/trans* isomerization and the millisecond incoherent timescale gives the rate of the process at longer times. The rate limiting process for human vision in moonlight is found to be low photon flux.

Qualitative remarks, of general interest, are provided at the end of the paper.

2. Theory

Our theoretical treatment of the photoisomerization is based on a one dimensional system with two electronic states (see Fig. 1a) connecting the *cis* and *trans* configurations, coupled through a strength parameter η to a "bath" that models the effects of the remaining degrees of freedom and of the external environment [15]. Isomerization occurs via rotation about an angle α. The interaction potential between the system and the coherent external field $E(t)$ is treated by means of the dipole approximation. In the case of low level incoherent light, $E(t) = 0$ and a second bath describing the incoherent light is included. That is, our Hamiltonian is

$$H_{\rm T} = H_{\rm S} - \mu E(t) + H_{\rm Ienv} + H_{\rm env} + H_{\rm Irad} + H_{\rm rad}, \tag{1}$$

where $H_{\rm S}$ is system Hamiltonian, μ is transition dipole moment of the system, $E(t)$ is electric field of the laser pulse, $H_{\rm env}$ is the environment Hamiltonian, $H_{\rm Ienv}$ is the interaction Hamiltonian between the system and environment, $H_{\rm rad}$ describes blackbody radiation, and $H_{\rm Irad}$ is interaction Hamiltonian between the system and the radiation field.

Eigenstates $|i\rangle$ of the system $H_{\rm S}$ satisfy

$$H_{\rm S}\,|i\rangle = \lambda_i\,|i\rangle\,, \tag{2}$$

and the density matrix accounted with evolution of the (system + bath) is denoted $\rho_{\rm T}$. The system density matrix is $\rho = {\rm Tr}_{\rm B}\rho_{\rm T}$, where ${\rm Tr}_{\rm B}$ denotes a trace over the bath. The time propagation of the density matrix elements of the system $\rho_{ij}(t) = \langle i|\,\rho(t)\,|j\rangle$ is assumed to be described by Redfield theory within a secular approximation [16, 17, 18, 19] as,

$$\begin{aligned}
\frac{\partial}{\partial t}\rho_{ii} &= \sum_{j\neq i} w_{ij}\rho_{jj} - \rho_{ii}\sum_{j\neq i} w_{ji} && (3)\\
&- i\frac{E(t)}{\hbar}\sum_m \left[\rho_{im}(t)\,\mu_{mi} - \mu_{im}\rho_{mi}(t)\right] && (4)\\
\frac{\partial}{\partial t}\rho_{ij} &= -i\omega_{ij}\rho_{ij}(t) - \gamma_{ij}\rho_{ij}(t) && (5)\\
&- i\frac{E(t)}{\hbar}\sum_m \left[\rho_{im}(t)\,\mu_{mj} - \mu_{im}\rho_{mj}(t)\right] \qquad (i\neq j), && (6)
\end{aligned}$$

where $w_{ji} = \Gamma^{+}_{ijji} + \Gamma^{-}_{ijji}$ is transition probability per unit time from ith to jth eigenstate of $H_{\rm S}$, and $\gamma_{ij} = \sum_k \left(\Gamma^{+}_{ikki} + \Gamma^{-}_{jkkj}\right) - \Gamma^{+}_{jjii} - \Gamma^{-}_{jjii}$ is dephasing rate. Here,

$$\begin{aligned}
\Gamma^{+}_{ljik} &= \frac{1}{\hbar^2}\int_0^\infty d\tau e^{-i\omega_{ik}\tau}\left\langle H_{{\rm Ienv}_{\rm lj}}(\tau)\,H_{{\rm Ienv}_{\rm ik}}\right\rangle_{\rm env}\\
&+ \frac{1}{\hbar^2}\int_0^\infty d\tau e^{-i\omega_{ik}\tau}\left\langle H_{{\rm Irad}_{\rm lj}}(\tau)\,H_{{\rm Irad}_{\rm ik}}\right\rangle_{\rm rad} && (7)\\
\Gamma^{-}_{ljik} &= \left(\Gamma^{+}_{kijl}\right)^*, && (8)
\end{aligned}$$

where the brackets $\langle\ldots\rangle_{\rm B}$ represent a trace over degrees of freedom in B, where B is either the environment "env" or the incoherent radiation field "rad", and $H_{\rm IB}(t) = e^{iH_{\rm B}t/\hbar}H_{\rm IB}e^{-iH_{\rm B}t/\hbar}$.

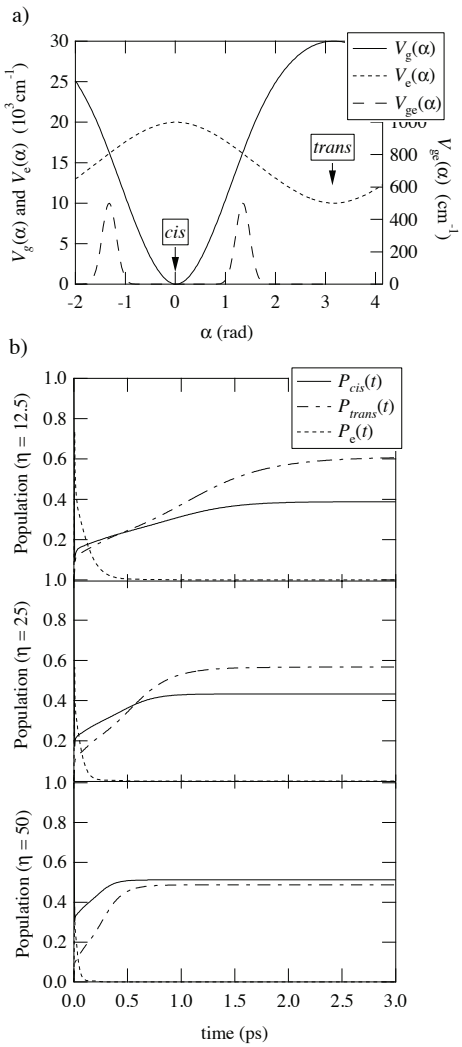

Figure 1: a) Potential energy surfaces for the two state model for *cis* to *trans* photoisomerization. The solid curve and dotted curve show diabatic potentials V_g and V_e, respectively. The dashed curve shows a coupling potential between two diabatic electronic states. b) Time propagation of cis and trans populations under a short intense pulse for different values of η. P_{cis} is the population in the range $-\frac{\pi}{3} \leq \alpha \leq \frac{\pi}{3}$ on V_g, P_{trans} is that in the range $-\pi \leq \alpha \leq -\frac{2\pi}{3}$ on V_e, and $P_e = 1 - P_{cis} - P_{trans}$. Note that in Panels b and c, the very short time dynamics, which includes the excitation from the *cis*, is not evident due to the short time over which it occurs.

The system Hamiltonian $H_{\rm S}$ is given in terms of two diabatic electronic states by

$$H_{\rm S} = \begin{pmatrix} T + V_{\rm g}(\alpha) & V_{\rm ge}(\alpha) \\ V_{\rm eg}(\alpha) & T + V_{\rm e}(\alpha) \end{pmatrix}, \tag{9}$$

where $T = -\frac{\hbar^2}{2m}\frac{\partial^2}{\partial\alpha^2}$ is the kinetic energy, $V_{\rm g}(\alpha)$ and $V_{\rm e}(\alpha)$ are the potential energy surfaces in ground and excited electronic state, and $V_{\rm ge}(\alpha) = V_{\rm eg}(\alpha)$ is the coupling potential between ground and excited states (see Fig. 1a).

The molecular environment is described as a set of harmonic oscillators of frequency ω'_n and the system–environment coupling is $H_{\rm Ienv} = Q\sum_n \hbar\kappa_n\left(b_n^\dagger + b_n\right)$, where $b_n^\dagger$ and b_n are the creation and annihilation operators pertaining to the nth harmonic oscillator. The operator Q is a diagonal 2×2 matrix with $\cos\alpha$ on the diagonal, and the coupling constants κ_n and spectrum of the bath are chosen in accord with an Ohmic spectral density $J(\omega) = 2\pi\sum_n \kappa_n^2\delta(\omega-\omega'_n) = \eta\omega e^{-\omega/\omega_c}$, where the strength of the system–environment coupling is determined by the dimensionless parameter η, and $\omega_c = 300\,{\rm cm}^{-1}$. After some algebra, we obtain first term of Eq. 7 as,

$$\begin{aligned}\frac{1}{\hbar^2}\int_0^\infty d\tau e^{-i\omega_{ik}\tau}\left\langle H_{{\rm Ienv}_{\rm ij}}(\tau)\,H_{{\rm Ienv}_{\rm ik}}\right\rangle_{\rm env} &= \frac{1}{2\pi}Q_{lj}Q_{ik}\int_0^\infty d\tau\int_0^\infty d\omega J(\omega)\cdot \\ &\cdot\left\{[\bar n(\omega)+1]\,e^{-i(\omega_{ik}+\omega)\tau} + \bar n(\omega)\,e^{-i(\omega_{ik}-\omega)\tau}\right\},\end{aligned} \tag{10}$$

where $\bar n(\omega) = \{\exp(\hbar\omega/k_bT)-1\}^{-1}$ is the Bose distribution at temperature $T = 300\,{\rm K}$, $\omega_{ji} = \left(\lambda_j-\lambda_i\right)/\hbar$, and λ_i is an eigenenergy of $H_{\rm S}$.

As a typical situation of scotopic vision, we consider moonlight, which is well characterized as a blackbody source at 4100 K [20]. This incoherent radiation field can also be described as a set of harmonic oscillators of frequency ω''_n and the system–radiation field coupling is treated by means of dipole approximation as,

$$H_{\rm Irad} = \mu\sum_{\mathbf{k}} i\sqrt{\frac{\hbar\omega''_k}{2\epsilon_0 V}}\sin\theta\left\{a_{\mathbf{k}}\exp\left(i\mathbf{k}\cdot\mathbf{r}\right) - a_{\mathbf{k}}^\dagger\exp\left(-i\mathbf{k}\cdot\mathbf{r}\right)\right\}, \tag{11}$$

where $\mathbf{k}$ is a wave number vector, ϵ_0 is the permittivity of vacuum, $\mathbf{r}$ is a position inside of a cavity, V is volume of the cavity, and θ is an angle between the transition dipole moment vector and $\mathbf{k}$ [21]. By assuming the large cavity limit the summation of $\mathbf{k}$ can be replaced with integrals, and second term of Eq. 7 is written as,

$$\begin{aligned}\frac{1}{\hbar^2}\int_0^\infty d\tau e^{-i\omega_{ik}\tau}\left\langle H_{{\rm Irad}_{\rm ij}}(\tau)\,H_{{\rm Irad}_{\rm ik}}\right\rangle_{\rm rad} &= C\frac{\mu_{lj}\mu_{ik}}{2\hbar\epsilon_0\pi^3}\int_0^\infty d\tau\int_0^\infty dk\int_0^{\frac{\pi}{2}} d\theta\int_0^{\frac{\pi}{2}} d\phi k^2\sin\theta^3\cdot \\ &\cdot\left[\left(\bar n\left(\omega''_k\right)+1\right)e^{-i\left(\omega''_k+\omega_{ik}\right)\tau} + \bar n\left(\omega''_k\right)e^{i\left(\omega''_k-\omega_{ik}\right)\tau}\right].\end{aligned} \tag{12}$$

A component of the imaginary part of Eq. 12 describes the Lamb shift. The integration with respect to k does not converge, and this difficulty can be avoided by renormalization theory [22]. However, since the effect of Lamb shift is generally less than $0.1\,{\rm cm}^{-1}$, the divergent term in Eq. 12 is neglected in this paper. The coefficient C in Eq. 12 is introduced to adjust density of blackbody radiation to that of light incident on our retina. Specifically, by assuming that one is looking at a surface lit by moonlight, with a color temperature of 4100 K and a luminance $L\,{\rm Cd\cdot m}^{-2}$, the ratio of the intensity of light falling on the retina over the light falling on the cornea as 0.5, the pupil area $3.8\times10^{-5}\,{\rm m}^2$, and the distance from the lens to the retina of 0.0167 m, we obtain $C = L/4.0\times10^{10}$. Here, a conversion from luminous flux in Cd·sr to radiant flux in ${\rm W\cdot m}^{-1}$ was done by using the spectral luminous efficiency function for scotopic vision [23].

From Eqs. 10 and 12, we obtain the transition probability in Eq. 3 as,

$$w_{ji} = \begin{cases} CB_{ji}W\left(-\omega_{ji}\right) + A_{ji} + \left|Q_{ji}\right|^2 J\left(-\omega_{ji}\right)\left[\bar n\left(-\omega_{ji}\right)+1\right] & \text{for } \omega_{ji}<0 \\ CB_{ji}W\left(\omega_{ji}\right) + \left|Q_{ji}\right|^2 J\left(\omega_{ji}\right)\bar n\left(\omega_{ji}\right) & \text{for } \omega_{ji}>0 \end{cases}, \tag{13}$$

where A_{ij} and B_{ij} are Einstein A and B coefficient in between the ith and jth eigenstate of $H_{\rm S}$, and $W(\omega)$ is the Planck's energy density. The dephasing ratio γ_{ij} in Eq. 5 is evaluated by numerical integration of Eq. 10.

Two comments are in order. First, a small amount of coherence is introduced into the moonlight case due to the fact that the field is turned on at $t = 0$. Second, note that neither in the case of coherent nor in the case of incoherent excitation is the return of the *trans* configuration to the *cis* included is these studies. This is justified by the fact that within rhodopsin the *trans* retinal is known [24] to leave the protein pocket, and is only restored to the protein pocket by other protein subunits over a long time ($\approx$ 1 sec or so). Hence, these time scales are not expected to affect the conclusions arising from these computations.

3. Results and Discussion

Figure 1b shows the time propagation of molecular populations under a typical laser pulse of time duration 5 fs, amplitude 4×10^9 V/m, and a carrier frequency of $2 \times 10^4\,\mathrm{cm}^{-1}$ that is resonant with the excitation to the electronic excited state around the Franck–Condon region. The transition dipole moment, set at 10 Debye, corresponds to an oscillator strength $f \approx 1$. At time $t = 0$, the *cis* population $P_{cis}(t = 0)$ is almost unity, and after $t = 10$ fs, probability is created in the excited state. Each panel in the Fig. 1b shows the relaxation process with a different degree of system–environment coupling: $\eta = 12.5$, 25 and 50. Evident is the fact that the *trans* yield is lower, and the isomerization is faster, with increasing coupling η to the bath. We note that the time scale of the reaction in Fig. 1 is in accord with that observed experimentally using coherent light excitation of rhodopsin, i.e. on the order of 200 fs [1, 2].

To assure that these results reflect laser coherence as opposed to laser intensity, the computation was repeated with a significantly reduced laser intensity (a maximum of 5×10^7 V/m). Here the product population dynamics, confirmed to be in the linear regime and shown in Fig 2, is seen to behave the same as that in Fig. 1. Hence, a comparison of these results with the dynamics in the weak incoherent light, below, is justifiable.

By contrast to the results above, the time dependence of the molecular populations for the case of excitation by incoherent light is shown in Fig. 3. Here we examine the problem in a context relevant to realistic biological systems. As seen in Fig. 3, for all η the rate of increase of P_{trans} is linear in time after a time that we denote as $t_c(\eta)$. Subsequent to that time the slope of P_{trans} vs. t is $s = 9.4 \times 10^{-8}\,\mathrm{s}^{-1}$, corresponding to a *cis/trans* isomerization timescale of almost one year. Note that the slope s is independent of the speed of photoisomerization observed under pulsed laser conditions, as evidenced by the fact that it is independent of η. Rather, this rate of transformation is dictated by the photon flux, which is the rate limiting reagent in the process. By contrast, the time t_c, which corresponds well to the time scale of photoisomerization under the laser pulse, relates directly to η as $t_c\eta \approx 20$ ps. For example, for the case of $\eta = 12.5$, $t_c = 1.5$ ps, in accord with Fig. 1b.

Figure 3b shows the time dependence of P_{trans} as a function of the luminance L of the incoherent light source. The slope s is seen to be proportional to the luminance L as $s/L \approx 3.1 \times 10^{-6}\,\mathrm{Cd}^{-1}\cdot\mathrm{m}^2\cdot\mathrm{s}^{-1}$.

Since the isomerization of only a few molecules are necessary to induce hyperpolarization in a rod cell [14, 10], we compute P_3, the probability that at least three from among all of the *cis* molecules in a rod cell are converted to *trans*. The probability would then correspond to the rate of our initial visual process under moonlight conditions. The probability $P_3(t)$ that at time t at least three from among N molecules are *trans* is given by $1 - p_0 - p_1 - p_2$, where

$$p_n = C_N^n p^n (1 - p)^{N-n} \tag{14}$$

is a probability that n from among N molecules are converted to *trans*. Here, $p = P_{trans}(t)$ is the probability that a molecule is *trans* at time t, and C_N^n is the binomial coefficient. For the case of vision, we take the number of rhodopsin molecules in a rod cell to be $N = 4{\times}10^9$ [25], and assume that the time dependence of P_{trans} maintains a constant slope s until $t = 25$ msec. The resultant P_3 values are shown in Fig. 4, where the time scale to obtain at least three *trans* molecules is on the order of a few tens of milliseconds. This finding is consistent with experimental time scales of 10 msec for dim flash response of a rod cell [10]. We note, as in the previous results, that the speed of photoisomerization under pulsed laser conditions is seen to bear no relation to the far longer time scales associated with the evolution of probability P_3, since the photon flux is rate-determining in the latter case. Note further that the times at which $P_3(t)$ reaches the value of 0.5, a measure of the biological response, is virtually a linear function of the irradiance.

Thus far, molecular time evolution in incoherent light was considered using the Redfield approach. We also find that the population transfer can be modeled analytically by solving the simple three state model with the four reaction rates shown in Fig. 5. A comparison with the computed Fig. 3 gives excellent results. Here, states A, B, and C

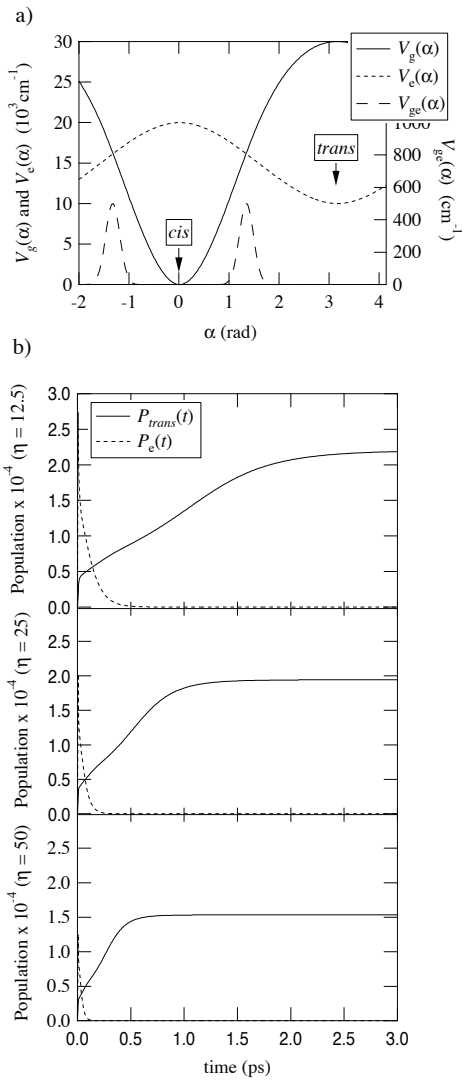

Figure 2: As in Fig. 1 but with significantly reduced laser intensity.

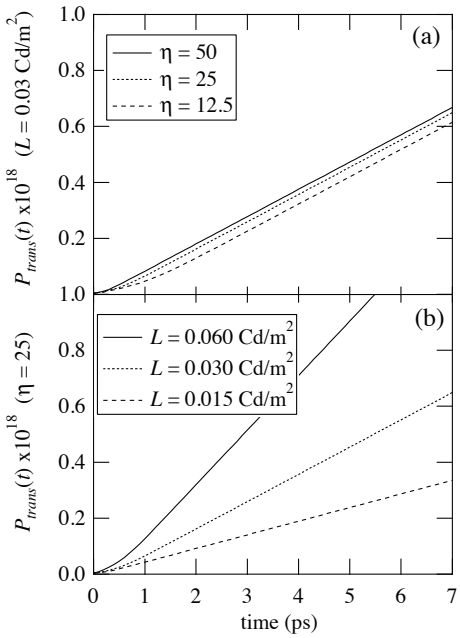

Figure 3: a) Time dependence of P_{trans} for three η values with incoherent light luminescence $L = 0.03\,\mathrm{Cd{\cdot}m^{-2}}$. b) Time dependence of P_{trans} for various values of L, with system–environment coupling $\eta = 25$. In all cases there is a deviation from strictly linear behavior at the early times that corresponds to timescales of isomerization dynamics.

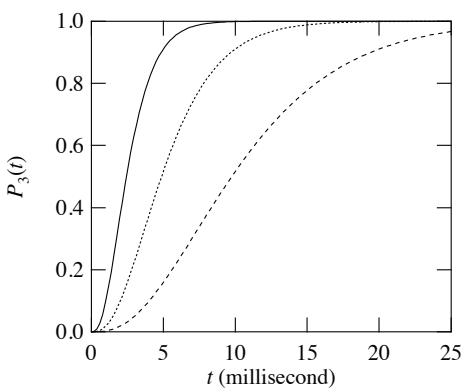

Figure 4: Time dependence of the probability P_3 that at least three from among $4{\times}10^9$ *cis* molecules become *trans* for various values of L: 0.060 Cd/m^2 (solid); 0.030 Cd/m^2 (dotted); 0.015 Cd/m^2 (dashed).

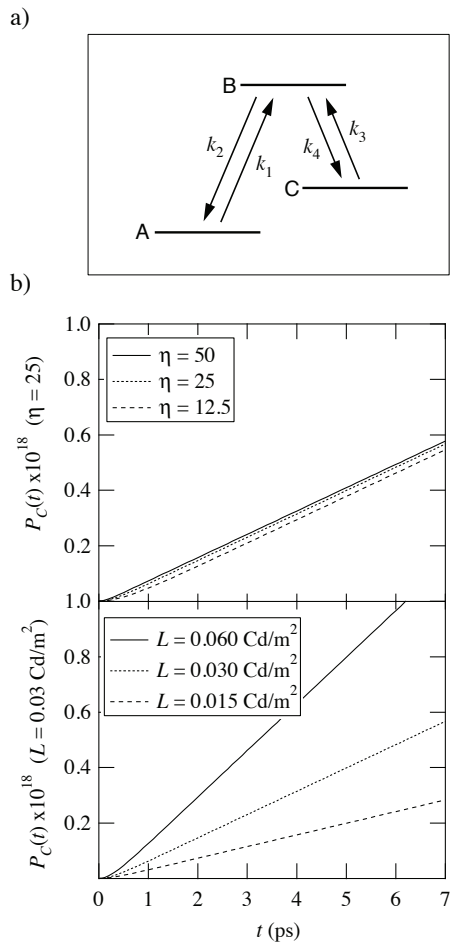

Figure 5: a) Three states model with reaction rates k_1, k_2, k_3, and k_4. Time propagation of P_C for each luminance L and strength parameter of system–environment coupling η. Compare with results shown in Fig. 3.

represent *cis*, excited, and *trans* conformations of the molecule, respectively. The values of k_2 and k_4 correspond to rates of population transfer from P_e to P_{cis} and P_{trans}, which are mainly caused by the system–environment coupling. Values obtained from the coherent pulse studies of Fig. 1 give $k_2 = k_4 = 0.08\eta\,\mathrm{ps}^{-1}$. The k_1 and k_3 represent rates of population transfer from P_{cis} and P_{trans} to P_e, caused by both system–environment coupling and photoabsorption. The rates of system–environment coupling can be assigned using detailed balance, and the rates of photoabsorption are given by the Einstein transition probability from the electronic ground state to the electronic excited state. In the case of k_1, the primary contribution is photoabsorption, giving $k_1 = BW = L \times 5.6 \times 10^{-6}\,\mathrm{Cd}^{-1}\cdot\mathrm{m}^2\cdot\mathrm{s}^{-1}$, where B is the Einstein B coefficient, and W is density of energy of the radiation field. The densities of the field used in Fig. 5 correspond to the luminescence values used in Fig. 3 [26]. On the other hand, in the case of k_3, the dominant term is system–environment coupling, and we obtain $k_3 = k_4 \times 1.87 \times 10^{-9}$. With the resultant k_1, $k_3 << k_2$, k_4, the rate equations give the reaction rate for isomerization under incoherent light as $k_1/2 = BW/2$. Further, these equations establish the existence of a linear region for P_{trans} vs. t with an η independent slope $s = k_1/2$ after a time $t_c = 3/(k_2 + k_4)$, relating the rate approach to both the computed coherent and incoherent results.

We note that the reaction rate obtained by the three state model is ≈10 % smaller than that given by the Redfield equation. The difference mainly comes from the simplifying assumption that $k_2 = k_4$, and the evaluation of the rate of photoabsorption at the torsional angle α set to zero. Nonetheless, all of the trends seen in the Redfield computed results are also evident in the rate equation results.

4. Summary

We have presented a unified theoretical model of photoisomerization under both a coherent light source such as a femtosecond laser pulse and an incoherent light source such as moonlight. The exact response observed reflects the combined effect of the characteristics of the radiation field and the underlying dynamics. To consider the specific case of retinal photoisomerization we introduced a minimal model of the isomerization process that gives the same timescale as the femtosecond laser experiment. Using this model we showed that the time scale for photoisomerization under coherent light corresponds to the initial rise time t_c of the photoisomerization under incoherent light. The latter arises due to the sudden turn-on of the incoherent light at $t = 0$.

Significantly, the overall timescale for the natural incoherent process, excitation under weak light conditions, was shown to be determined by the low photon flux in the source, as opposed to a specific property associated with molecular coherence. Further, we introduced a simple three state model that incorporates all of the relevant rates obtained from both the femtosecond and millisecond time domains.

This approach provides a connection between the time domain of the femtosecond laser experiment on retinal in rhodopsin and that of biologically relevant response time scales in human vision.

5. Acknowledgment

This work was carried out with partial support from NSERC Canada and from the AFOSR under grant FA9550-10-1-0260. We thank Professor R.J. Dwayne Miller for comments on an earlier version of this manuscript.

6. References

[1] Q. Wang, W. Schoenlein, L. Peteanu, R. Mathies, C. Shank, Science 266 (1994) 422.
[2] H. Kandori, Y. Shichida, T. Yoshizawa, Biochemistry (Moscow) 66 (2001) 1483.
[3] T. Kobayashi, T. Saito, H. Ohtani, Nature 414 (2001) 531.
[4] V. Prokhorenko, A. Nagy, S. Waschuk, L. Brown, R. Birge, R. Miller, Science 313 (2006) 1257.
[5] M. Spanner, C. Arango, P. Brumer, J. Chem. Phys in preparation.
[6] W. Parsons, Modern Optical Spectroscopy, Springer, New York, 2009.
[7] M. Cho, Two Dimensional Optical Spectroscopy, CRC Press, New York, 2009.
[8] A. Ishizaki, T. Calhoun, G. Schlau-Cohen, G. Fleming, Phys. Chem. Chem. Phys. 12 (2010) 7319.
[9] E. Collini, C. Wong, K. Wilk, P. Curmi, P. Brumer, G. Scholes, Nature 463 (2010) 644.
[10] N. Sperelakis (Ed.), Cell Physiology Source Book, 2nd Edition, Academic Press, San Diego, 1998, Ch. 47.
[11] X.-P. Jiang, P. Brumer, J. Chem. Phys. 94 (1991) 5833.
[12] X.-P. Jiang, P. Brumer, Chem. Phys. Lett. 180 (1991) 222.

[13] T. Mancal, L. Valkunas, New J. Phys. 12 (2010) 065044.
[14] F. Rieke, D. Baylor, Rev. Mod. Phys. 70 (1998) 1027.
[15] Models of this type have also proven enlightening in a variety of other studies of open system isomerization dynamics. See, e.g. K. Hoki and P. Brumer, Phys. Rev. Lett., 95, (2005) 168305 and K. Hoki and P. Brumer, Chem. Phys. Lett. 468, (2009), 23.
[16] R. Redfield, IBM J. Res. Dev. 1 (1957) 19.
[17] K. Blum, Density Matrix Theory and Applications, Plenum Press, New York, 1981.
[18] V. May, O. Kühn, Charge and Energy Transfer Dynamics in Molecular Systems, Wily-VCH, Berlin, 2000.
[19] W. Pollard, A. Felts, R. Friesner, Adv. Chem. Phys. 93 (1996) 77.
[20] H. Davison, Physiology of the Eye, 5th Edition, Macmillan Press, London, 1990.
[21] R. Loudon, The Quantum Theory of Light, 2nd Edition, Oxford University Press, 1983.
[22] W. Louisell, Quantum Statistical Properties of Radiation, John Wiley & Sons, 1990.
[23] ISO/CIE 10527 (1991) CIE Standard Colorimetric Observers.
[24] V. Prokhorenko (private communication).
[25] C. Graymore (Ed.), Biochemistry of the Eye, Academic Press, London, 1970, Ch. 9.
[26] Here $W = 2.5 \times 10^{-11} w(\omega) L$, where the coefficient is estimated by using the radius of pupil, the distance between the lens and a surface, etc., L is luminance of the surface in Cd·m^{-2}, and $w(\omega)$ is the black body energy density at 4100K. Here, W and $w(\omega)$ have units of Joule·sec·m^{-3}.